ACS Catalysis

Subscriber access provided by The Chinese University of Hong Kong

Article

Nature of the Entire Range of Rare-Earth Metal Based Cationic Catalysts for Highly Active and Syndioselective Styrene Polymerization

Fei Lin, Xingbao Wang, Yupeng Pan, Meiyan Wang, Bo Liu, Yi Luo, and Dongmei Cui

ACS Catal., **Just Accepted Manuscript** • DOI: 10.1021/acscatal.5b02334 • Publication Date (Web): 23 Nov 2015

Downloaded from http://pubs.acs.org on November 25, 2015

Just Accepted

"Just Accepted" manuscripts have been peer-reviewed and accepted for publication. They are posted online prior to technical editing, formatting for publication and author proofing. The American Chemical Society provides "Just Accepted" as a free service to the research community to expedite the dissemination of scientific material as soon as possible after acceptance. "Just Accepted" manuscripts appear in full in PDF format accompanied by an HTML abstract. "Just Accepted" manuscripts have been fully peer reviewed, but should not be considered the official version of record. They are accessible to all readers and citable by the Digital Object Identifier (DOI®). "Just Accepted" is an optional service offered to authors. Therefore, the "Just Accepted" Web site may not include all articles that will be published in the journal. After a manuscript is technically edited and formatted, it will be removed from the "Just Accepted" Web site and published as an ASAP article. Note that technical editing may introduce minor changes to the manuscript text and/or graphics which could affect content, and all legal disclaimers and ethical guidelines that apply to the journal pertain. ACS cannot be held responsible for errors or consequences arising from the use of information contained in these "Just Accepted" manuscripts.

ACS Publications

ACS Catalysis is published by the American Chemical Society. 1155 Sixteenth Street N.W., Washington, DC 20036

Published by American Chemical Society. Copyright © American Chemical Society. However, no copyright claim is made to original U.S. Government works, or works produced by employees of any Commonwealth realm Crown government in the course of their duties.

Nature of the Entire Range of Rare-Earth Metal Based Cationic Catalysts for Highly Active and Syndioselective Styrene Polymerization

Fei Lin[1,2], Xingbao Wang[3], Yupeng Pan[1,2], Meiyan Wang[4], Bo Liu,[1]* Yi Luo,[3]* and Dongmei Cui [1]*

[1]State Key Laboratory of Polymer Physics and Chemistry, Changchun Institute of Applied Chemistry, Chinese Academy of Sciences, Changchun 130022, China

[2]University of the Chinese Academy of Sciences, Changchun Branch, Changchun 130022, China

[3]State Key Laboratory of Fine Chemicals, School of Pharmaceutical, Science and Technology, Dalian University of Technology, Dalian 116024, China

[4]Institute of Theoretical Chemistry, State Key Laboratory of Theoretical and Computational Chemistry, Jilin University, Changchun 130022, China

*Corresponding authors: FAX +86 431 85262774; e-mail dmcui@ciac.ac.cn; liubo@ciac.ac.cn; luoyi@dlut.edu.cn.

ABSTRACT By merit of the steric bulkiness and the η^5/κ^1-constrained-geometry-configuration (CGC) geometry, the pyridyl-methylene-fluorenyl stabilized entire range of rare-earth metal bis(alkyl) complexes, (Flu-CH_2-Py)Ln(CH_2SiMe_3)$_2$(THF)x (Flu = fluorenyl; Py = pyridyl; **1**: Ln = Sc, x = 0; **2**–**11**: Lu, Tm, Er, Ho, Y, Dy, Tb, Gd, Nd, Pr, x = 1) and mono(alkyl), (Flu-CH_2-Py)$_2$La(CH_2SiMe_3)(THF) (**12**), have been successful achieved for the first time via the sequential salt metathesis reactions. Activated by [Ph_3C][$B(C_6F_5)_4$] and Al^iBu_3, complexes **1**–**9** showed high activity and perfect syndioselectivity for styrene polymerization, while the large Nd and Pr attached precursors **10** and **11** exhibited slightly dropped syndioselectivity but rather low activity, and the monoalkyl La precursor **12** was completely inert. The activity increased with the decrease of the rare-earth metal size, in striking contrast to the literatures that a large sized metal facilitates a high activity, which was also not a result of enthalpic effect ($\Delta H^\ddagger$) or entropic effect ($\Delta S^\ddagger$) according to Eyring plots. The types of the organoborates and the aluminum alkyls, the electron-donors and the polarity of reaction medium, which affected the coordination of styrene to the active species, aroused significantly different catalytic activity, indicating that styrene coordination played the key role in

the polymerization process. Based on this, the DFT calculation of the active species in the model of $[(\text{Flu-CH}_2\text{-Py})\text{Ln}-\text{nC}_{17}\text{H}_{19})]^+$ revealed whenever the orbitals of the pyridyl-methylene fluorenyl ligand overlapped with those of the rare-earth metals, the LUMO energy of the active species was lowered and thus the catalytic activity was high. Therefore the LUMO energy of the active species could be adopted as a potential criterion to estimate the activity of a catalytic system for styrene polymerization. This work reveals for the first time the power of the pyridyl-methylene fluorenyl ligand and the nature of the factors influencing the catalytic performances.

INTRODUCTION

The cationic group 3 metal alkyl complexes have reached an upsurge of research interests in the past two decades not only because they possess versatile catalytic peroformances upon activation with MAO, or aluminum alkyls/organoborates for the olefin (co)polymerizations, but also their potential of generating marvelous catalysis when changing the electron donating or withdrawing substituents and the steric bulkiness of the ligands, since no other metals have so variable electronics ($d^{0-1}-f^{0-14}$) and sterics (ionic radius: 0.89 − 1.17 Å).[1] As the 4f electrons are believed not involve in ligand or substrate bonding, the relative reactivity of these rare-earth metals based catalytic precursors is expected to be determined mainly by the metal ionic radius. However, to illustrate this has been a challenging project of the academic area, since any one ligand is difficult to cover the entire range of rare-earth metals, in particular the large ones for which the bis- or tris-ligands supported complexes are usually isolated as the major products arising from ligand disproportionation. Okuda found that the dicationic rare-earth metal (heavier than Tb) alkyl species without attaching to any ligands displayed an increasing activity for ethylene polymerization with increase of the ionic radius.[2] Hessen discovered the amidinate ligand was fit for the full range of cationic rare-earth metal monoalkyl species, of which the yttrium species exhibited the highest activity.[3] With regard to the polar monomer, Yasuda also found the catalytic activity of $\text{Cp*}_2\text{LnMe(THF)}$ increased with the metal ion size towards the group transfer coordination polymerization (GTP) of MMA.[4] It is the commonly adopted explanation that the large sized active metal center facilitates the polymerization owing to it providing a more opening coordination sphere, which, however, usually lacks scrutinized investigation. Very recently, Rieger reported the catalytic activity of Cp_3Ln being accelerated by decreasing the metal radius for GTP of vinylphosphonates, who elegantly explained and proved the origin being that the steric demanding (small) active metal center changed slightly the $\Delta S^{\ddagger}$ of the transition state while the less steric (large) active metal center dramatically decreased the $\Delta S^{\ddagger}$ but the $\Delta H^{\ddagger}$ remained constantly in both cases.[5] The contradictive picture leaves the investigation of the following questions open: What is the nature concerning the relationship between the polymerization activity and the rare-earth catalyst? Does the ligand play any role in it?

Syndiotactic polystyrene (sPS) is a promising engineering plastics due to its high melting point, rapid crystallization ability, high tensile modulus, low dielectric constant and excellent resistance to heat and chemicals.[6] The most efficient catalytic systems towards syndiotactic styrene polymerization belong to the group 4 titanium complexes.[7] In contrast, the group 3 rare-earth metal complexes are always inert to this polymerization until 2004 Carpentier reported the distinguished catalytic activity (1710 $Kg_{(sPS)}\cdot mol_{(Ln)}^{-1}\cdot h^{-1}$) of the netural allyl *ansa*-neodymocene catalyst, $[Flu\text{-}CMe_2\text{-}Cp]Nd(C_3H_5)(THF)$, for the bulk styrene polymerization at 60 ºC.[8] Almost at the same time, Hou reported the first cationic half-Sandwich scandium alkyl catalyst system, $[(C_5Me_4SiMe_3)Sc(CH_2SiMe_3)(THF)][B(C_6F_5)_4]$, with the excellent activity (13618 $Kg_{(sPS)}\cdot mol_{(Ln)}^{-1}\cdot h^{-1}$) and syndioselectivity (*rrrr* > 99 %).[9] Thereafter, many scandium precursors and only the scandium based precursors bearing cyclopentadienyl Cp,[10] linked Cp,[11] hetero-Cp,[12] indenyl[13] and fluorenyl[14] ligands unambiguously showed the similar distinguished performances, which seems to be attributed to the nature of the scandium, electronically close to titanium. We reported the pyridine-Cp* ligated lutetium allyl complex, $(C_5Me_4\text{-}C_5H_4N)Lu(C_3H_5)_2$,[15] which, under the activation of $[Ph_3C][B(C_6F_5)_4]$, can convert unprecedentedly 1000 equiv styrene into sPS within 1 min but its yttrium analogue displayed a much lower activity.

Therefore to explore the possibility of other lanthanide metals (much abundant and cheaper) based complexes to catalyze this stereospecific polymerization and the mechanism proceeded, is a great challenging but very attractive project from both academic and industry points of view.

Very recently, we found that the constrain-geometry-configuration (CGC) pyridine methylene fluorenyl (Py-CH_2-Flu) ligand stabilized rare-earth metal scandium, yttrium and lutetium precursors all showed distinguished activity and syndioselectivity.[16] Herein we report this powerful Py-CH_2-Flu ligand, by the merit of its steric bulkiness and the η^5/κ^1-CGC structure, not only can stabilize almost the entire range of rare-earth metal dialkyl species but also affect the catalytic activity of the central metals to such a degree that most of the rare-earth metal precursors upon activation show very high activity towards styrene polymerization except those of large metals such as Nd and Pr. DFT calculation, thermaldynamics (Eyring plots), and kinetics, as well as factors that may influence styrene coordination/insertion, were investigated to scrutinize the nature of the catalytic activity of styrene polymerization catalyzed by rare-earth metal complexes. Based this, a criterion to estimate the catalytic activity is proposed.

RESURTS AND DISCUSSION

Synthesis and Characterization of Complexes 1–12. Since the preparation of rare-earth metal alkyl complexes through deprotonating the ligand by the corresponding rare-earth metal tris(alkyl)s[16] was only available for metals of the sizes smaller than Tb,[2] complexes **1**–**12**, $[(\eta^5\text{-Flu-CH}_2\text{-Py})Ln(CH_2SiMe_3)_2(THF)_n]$, were prepared via metathesis reaction between the lithium salt of pyridyl-methylene functionalized fluorene (Flu-CH_2-Py)Li and $LnCl_3$ followed by the lithiation reaction with 2 equiv Me_3SiCH_2Li (Ln = Sc (**1**), yield: 85%; for **2**–**9**: Ln = Lu, Tm, Er, Ho, Y, Dy, Tb, Gd in 70-80% yields). However, complexes **10** (Ln = Nd) and **11** (Ln = Pr) were isolated at lower yields (**10**: 30 %; **11**: 25%) since the strong Lewis acidity and the large ionic radii of Pr and Nd metals led to unknown byproducts. The largest lanthanum attached complex **12** was isolated as a mono(alkyl) (yielding 10%) evidenced by the integral intensity ratio of 1:2 for the methylene protons from

$\mathrm{C}H_2\mathrm{SiMe}_3$ (two doublets centered at –1.70 and –2.82 ppm) and the pyridyl-methylene (doublet at 3.74 and 3.84 ppm) (Scheme 1). The scandium complex **1** is a solvent-free monomer while **2**–**11** bear one solvated THF molecule. The auxiliary ligand coordinates to the central metal ions in the η^5/κ^1-CGC mode via the Cp carbons and the dangling pyridyl nitrogen atom, combining two alkyl groups and a THF molecule to generate a tetrahedral geometry around the metal center (Figure 1 for complex **11** and Figures S1−S3 from complexes **4**, **9** and **10**). These molecular structures are consistent with those of yttrium and lutetium analogues reported previously.[16] With the ionic radius increasing, the $\mathrm{Ln{-}C_{alkyl}}$ bond lengths increase (Table S1), correspondingly, the $\mathrm{Cp_{cent}{-}Ln{-}N}$ bite angles decrease (Lu: 92.23°, Er: 91.53°,Gd: 89.75°, Nd: 88.20°, Pr: 88.58°), all are smaller than 95.4(3)° of $\mathrm{Cp_{cent}1{-}Y(1){-}N(1)}$ in the complex $\mathrm{NMe_2\text{-}C_6H_4\text{-}Cp^*Y(C_3H_6)_2}$[17] of an inert system to the styrene polymerization, suggesting that this pyridyl-methylene-Cp* CGC-ligand generates a relatively opening sphere around the metal center irrespective of the ionic size.

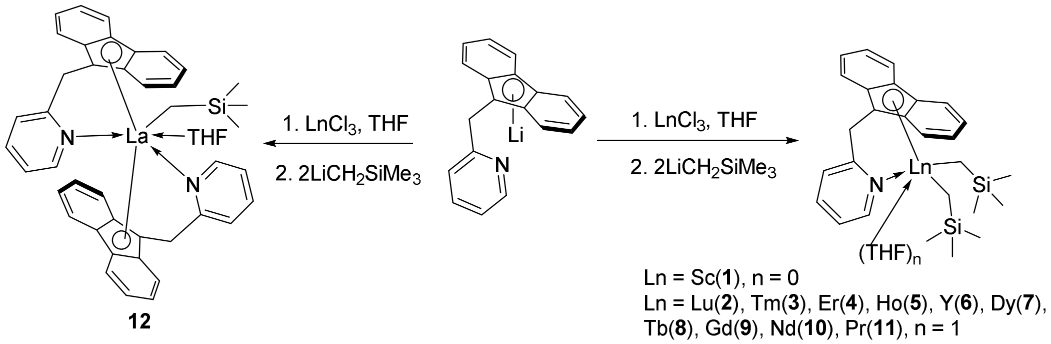

Scheme 1. Synthesis of rare earth metal alkyl complexes **1**–**12**.

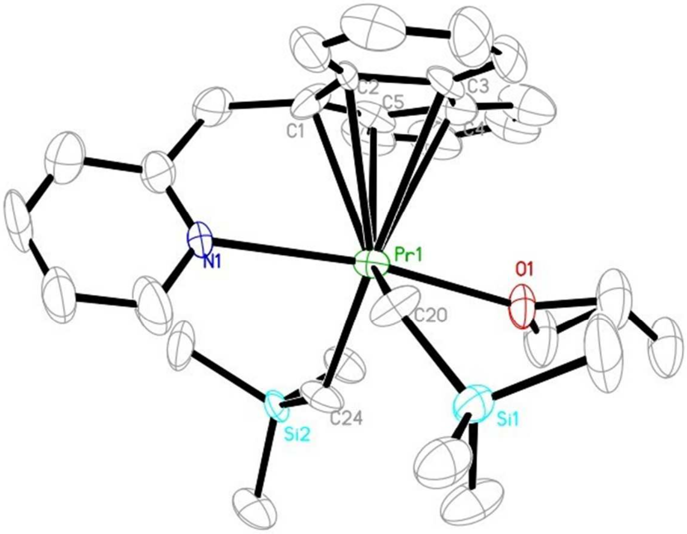

Figure 1. X-ray structure of complex **11** with thermal ellipsoids drawn at the 30% probability level. Hydrogens are omitted for clarity.

Styrene polymerization

All these complexes **1−12** in combination with $[Ph_3C][B(C_6F_5)_4]$ and $Al^{i}Bu_3$ were employed to catalyze styrene polymerization. The scandium complex **1** showed the highest activity to convert 10 000 equivalents styrene within 1 h to afford polystyrene with high molecular weight ($M_n = 82.3\times10^4$), narrow molecular weight distribution (PDI = 1.73) and perfect syndiotacticity (Table 1, entry 1), comparable to the literature.[16] Surprisingly, complexes **2−9** based on the lanthanide elements varying from Gd to Lu also displayed excellent performances with respect of the activity and syndioselectivity (Table 1, entries 2−14). The polymerization performed in the controlled manner that by using complex **5** as the catalyst changing the monomer-to-initiator ratio from 500 to 5000, the molecular weight of the resultant sPS almost increased proportionally, meanwhile the molecular weight distribution kept constant (Table 1, entries 5−8). In addition, such distinguished catalytic performances remained at elevated polymerization temperatures up to 80 ºC (Table 1, entry 9). However, the large metal Nd and Pr precursors **10** and **11** showed much lower activity albeit with the slightly dropped syndioselectivity while the lanthanum mono(alkyl) complex **12** was completely inert (Table 1, entries 15−17). This represented the rare example that most of the lanthanide elements based precursors displayed high activity towards syndioselective styrene polymerization, which might be attributed to the power of the ligand that provided a more opening coordination sphere by forming smaller bite angles with the rare-earth metals as compared to other CGC-rare-earth metal analogues (*vide supra*).

Table 1. Syndiospecific polymerization of styrene with rare-earth metal dialkyl complexes **1**−**12** activated by Al^{i}Bu$_3$ and [Ph$_3$C][B(C$_6$F$_5$)$_4$] under various conditions.[a]

Entry	Cat.	[St]/Ln	t(min)^b	Conv.(%)	sPS^c(%)	M_n^{d}×10^{-4}	M_w/M_n^{d}	T_m^{e}(℃)
1	Sc(**1**)	10000	60	＞99	>99	82.3	1.73	270
2	Lu(**2**)	10000	120	＞99	>99	67.3	1.60	270
3	Tm(**3**)	5000	30	＞99	>99	63.2	1.48	270
4	Er(**4**)	5000	30	＞99	>99	64.0	1.48	270
5	Ho(**5**)	500	5	＞99	>99	5.9	1.11	270
6	Ho(**5**)	1000	5	＞99	>99	10.7	1.15	270
7	Ho(**5**)	2500	10	＞99	>99	34.2	1.31	270
8	Ho(**5**)	5000	30	＞99	>99	60.4	1.52	270
9^f	Ho(**5**)	5000	30	＞99	>99	44.6	1.44	270
10	Ho(**5**)	10000	120	＞99	>99	68.9	1.62	270
11	Y(**6**)	10000	120	＞99	>99	67.7	1.81	270
12	Dy(**7**)	5000	90	＞99	>99	48.3	1.61	270
13	Tb(**8**)	5000	90	＞99	>99	46.2	1.60	270
14	Gd(**9**)	5000	90	＞99	>99	48.7	1.56	270
15	Nd(**10**)	5000	36 h	＞99	92	29.1	1.84	256
16	Pr(**11**)	5000	72 h	＞99	90	22.2	2.00	252
17	La(**12**)	1000	72h	--	--	--	--	--

[a] Polymerization conditions: Ln (10 μmol), [Cat]/Al^{i}Bu$_3$/[Ph$_3$C][B(C$_6$F$_5$)$_4$] = 1/10/1 (mol/mol/mol), when [St]/Ln⩽5000, toluene/monomer = 5/1 (v/v) ([St]/Ln = 10 000, toluene/monomer = 2.5/1 (v/v)), T_p = 15 °C, unless otherwise noted. [b] The time hasn't been optimized. [c] Measured by ^{1}H NMR and ^{13}C NMR spectroscopy in tetrachloroethane-d_2 at 125 °C. [d] Determined by GPC in 1,2,4-trichlorobenzene at 150 °C against polystyrene standard. [e] Determined by DSC. [f] T_p = 80 °C, toluene/monomer = 15/1 (v/v).

Kinetics Experiments

The polymerization catalyzed by all complexes under low conversions indicated the different polymerization rates of these complexes (Table S2), which could be explicated in more details by the kinetics study at low monomer concentrations. The linearship between ln{[St]$_0$/[St]$_t$} and time indicates the first-order dependence of polymerization rate on the styrene concentration catalyzed by complexes **1-11** (Figure S5). The observed rate constant (k_{obs}) for the catalyst based on Lu (**2**), Tm (**3**), Er (**4**), Ho (**5**), Y (**6**), Dy (**7**), Tb (**8**) or Gd (**9**) was 6.0×10^{-2}, 5.4×10^{-2}, 5.2×10^{-2}, 3.6×10^{-2}, 3.3×10^{-2}, 2.1×10^{-2}, 2.1×10^{-2} and 1.7×10^{-2} min^{-1} (Figure S4), respectively, which, roughly, was one order of magnitude lower than the scandium complex **1** (12.9×10^{-2} min^{-1}) and one order of magnitude higher than the neodymium complex **10** (0.2×10^{-2} min^{-1}) and praseodymium complex **11** (0.1×10^{-2} min^{-1}). Apparently, the order of the catalytic activity was well correlated with the effective ionic radius of the rare-earth metal: the smaller the metal size, the higher the catalytic activity of the corresponding complex (Figure 2). Noteworthy was that, the influence of the metal size on the activity was opposite to the previous reports by Okuda and Hessen for ethylene polymerization.[2,3] Yasuda also found the GTP activity of MMA increased with the increasing metal ion size although it was performed in different mechanism. These results are understandable since it is commonly accepted that large metal center usually provides opening coordination sphere to facilitate the polymerization, although it lacks a direct proof.[4] To date the only similar phenomena was reported by Rieger that the catalytic activity of $\mathrm{Cp_3Ln}$ was accelerated by decreasing the metal radius for GTP of vinylphosphonates, which was attributed to the steric demanding of the active metal center by changing the $\Delta S^{\ddagger}$of the transition state.[5] Hence, Eyring analyses of styrene polymerization using scandium complex (**1**), lutetium complex (**2**), holmium complex (**5**) and gadolinium complex (**9**) as catalytic precursors were carried out.

As shown in Table 2, the increase of metal ionic radius led to drop of the enthalpy $\Delta H^{\ddagger}$ (Lu(**2**) 59.5 kJ mol^{-1} > Ho(**5**) 56.8 kJ mol^{-1}> Gd(**9**) 55.8 kJ mol^{-1}) but enhance of $-T\Delta S^{\ddagger}$ (Lu(**2**) 30.6 kJ mol^{-1} < Ho(**5**) 35.1 kJ mol^{-1} < Gd(**9**) 36.6 kJ mol^{-1}). For the Sc (**1**) precursor, a much lower $\Delta H^{\ddagger}$ (40.6 kJ mol^{-1}) was observed but was accompanied by a much increased $-T\Delta S^{\ddagger}$ (48.7 kJ mol^{-1}). Therefore, it was hard to conclude that the increase of polymerization activity with the decreasing metal ionic radius was a result of enthalpic effects ($\Delta H^{\ddagger}$)[18] or entropic effects ($\Delta S^{\ddagger}$)[5]. This was inconsistent with the explanation drawn from the coordination-anionic GTP of vinylphosphates where the smaller metal size accelerated the activity by dramatically increasing the $\Delta S^{\ddagger}$ but keeping $\Delta H^{\ddagger}$ constant, because the crowded active metal center destabilized the transition state.[5]

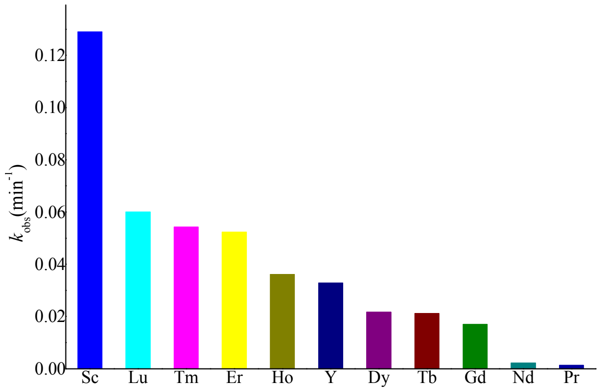

Figure 2. The observed rate constants (k_{obs}) of complexes **1**–**11** vs ionic radius (Ln (10 μmol), [Ln]/[Al^{i}Bu$_3$]/[Ph$_3$C][B(C$_6$F$_5$)$_4$]/[St] = 1/5/1/2000 (in mole), toluene/monomer = 30/1 (v/v), T_p = 15 °C)

Table 2. Activation enthalpy $\Delta H^{\ddagger}$, $\Delta S^{\ddagger}$ and k_{obs} for the catalytic systems based on Sc (**1**), Lu(**2**), Ho(**5**) and Gd(**9**) precursors.

Cat.	$k_{obs}\times10^2$ min	$\Delta H^{\ddagger}$(±2)(kJ·mol^{-1})	$\Delta S^{\ddagger}$(±2)(J • mol^{-1} • K^{-1})[a]
Sc(**1**)	12.9	40.6	–169.09
Lu(**2**)	6.0	59.5	–106.09
Ho(**5**)	3.6	56.8	–121.89
Gd(**9**)	1.7	55.8	–126.96

[a] The polymerization temperature T = 288 K.

Origin of High Catalytic Activity

The binary catalytic system **1**/[Ph$_3$C][B(C$_6$F$_5$)$_4$] was active towards styrene polymerization but **6**/[Ph$_3$C][B(C$_6$F$_5$)$_4$] was nearly inert under the same conditions (Table 3, entries 1 and 2). The major difference between the two systems was **6** containing a solvated THF molecule. As reported previously, THF could be abstracted easily by Al^{i}Bu$_3$ from the active metal center.[19] Indeed, addition 1 equiv Al^{i}Bu$_3$ to **6**/[Ph$_3$C][B(C$_6$F$_5$)$_4$] brought about an obvious increase of the activity (Table 3, entry 3). DFT calculation revealed that the barrier height for the styrene insertion process between the systems **6**/[Ph$_3$C][B(C$_6$F$_5$)$_4$] (13.0 kcal/mol) and

6/$[Ph_3C][B(C_6F_5)_4]/Al^iBu_3$ (11.4 kcal/mol) has no big difference as reported previously,[14] but the styrene coordination energy for the THF solvated former system (16.4 kcal/mol) is 15.7 kcal/mol higher than the late system without THF (0.7 kcal/mol) (Figure 3), suggesting that abstracting THF to generate a vacancy for monomer coordination is crucial to the polymerization.[8] Hence, THF presence or not is superficial phenomenon in structures, whether it impedes the coordination of monomer to the active metal center is the reason behind it. This can explain why some THF solvated systems are active to ethylene or styrene *etc* polymerizations.[9,17]

Replacing $[Ph_3C][B(C_6F_5)_4]$ by $[PhNMe_2H][B(C_6F_5)_4]$ to activate the scandium complex **1** generated a low active system (Table 3 entries 4 and 5). The reaction was monitored by ^1H NMR spectroscope technique to show that the methylene protons of $ScCH_2SiMe_3$ shift downfield (2.56: d, d, $^2J_{H,H}$ = 12 Hz; 1.94: d, $^2J_{H,H}$ = 15 Hz) as compared to that in **1**/$[Ph_3C][B(C_6F_5)_4]$,[20] meanwhile, the methyl protons of the resultant $PhNMe_2$ show at a higher field (2.85 ppm) than the free $PhNMe_2$ (2.95 ppm) because it coordinate to the Sc^{3+}.[21] Hence, Lewis base $PhNMe_2$ reduces the catalytic activity by occupying the active sites to obstruct styrene coordination.[8,22] The lowest activity of the system **1**/$[NEt_3H][B(C_6H_6)_4]$ might be ascribed to the interaction of the counter anion $B(C_6H_6)_4^-$ with the active metal center Sc^{3+} in a η^2(m,p)-mode (DFT simulation result, Figure S9)[23] thus blocking styrene coordination (Table 3, entry 6), which was further proved by the ^1H NMR spectrum analysis that the resonances of the four phenyl rings from $B(C_6H_6)_4^-$ are asymmetric and split into two sets.[24] Moreover, performing the polymerization in polar medium such as chlorobenzene (ε = 2.7), the catalytic activity of **6**/$[Ph_3C][B(C_6F_5)_4]/Al^iBu_3$ was dramatically improved than those in non-polar solvent such as hexane (ε = 0.06) (Table 3, entries 7−10), since the interaction between the cation and anion was weakened in the polar medium, leaving more space for styrene coordination.[25] The above results demonstrated that any factors influencing the coordination of styrene to the active metal center would arouse obvious change of the activity, suggesting it being the rate-limiting step.

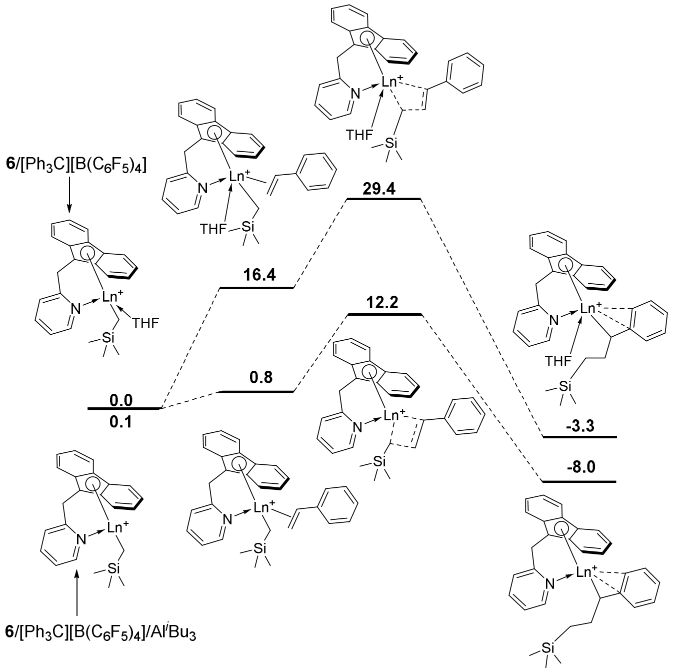

Figure 3. Free energy profiles calculated for coordination and insertion of styrene with THF in the activated species.

Table 3. Syndiospecific polymerization of styrene with rare-earth metal bisalkyl complexes **1** and **6** under various conditions.[a]

run	Cat./Borate/[Al]	Solvent	Time/min	conv.[b] (%)	M_n[c]($\times 10^{-4}$)	M_w/M_n[c]
1	**1**/$[Ph_3C][B(C_6F_5)_4]$/0	Toluene	2	10	9.8	1.40
2	**6**/$[Ph_3C][B(C_6F_5)_4]$/0	Toluene	3	-	-	-
3	**6**/$[Ph_3C][B(C_6F_5)_4]$/1.0	Toluene	3	8	7.0	1.15
4	**1**/$[Ph_3C][B(C_6F_5)_4]$/0	Chlorobenzene	0.5	44	11.9	1.45
5	**1**/$[PhNMe_2H][B(C_6F_5)_4]$/0	Chlorobenzene	0.5	6	11.1	1.54
6	**1**/$[NEt_3H][B(C_6H_5)_4]$/0	Chlorobenzene	30	5	1.0	1.74
7	**6**/$[Ph_3C][B(C_6F_5)_4]$/10.0	Hexane	4	6	2.0	4.60
8	**6**/$[Ph_3C][B(C_6F_5)_4]$/10.0	Hexane/Toluene[d]	4	21	6.9	1.97
9	**6**/$[Ph_3C][B(C_6F_5)_4]$/10.0	Toluene	4	49	16.4	1.19
10	**6**/$[Ph_3C][B(C_6F_5)_4]$/10.0	Chlorobenzene	4	71	23.8	1.26

[a] Polymerization conditions: Ln = 10 μmol, T_p = 15 °C, [Cat]/[St] = 1/2000 (entries 1-4) and 1/1000 (entries 5-10), solvent/monomer (v/v) = 20/1 (entries 1-4) and 10/1 (entries 5-1), according to the ^{13}C NMR spectroscopy of the afforded polymer in tetrachloroethane-d_2 at 125 °C, *rrrr* > 99%; [b] Calculated by weight; [c] Determined by GPC in 1,2,4-trichlorobenzene at 150 °C against polystyrene standard; [d] Hexane/toluene = 1:1 (v/v).

As far as styrene coordination polymerization is concerned, the electron donation π–C=C bonding to the empty orbital of the active metal center is generally dominant. Thus the energy gap (ΔE) between the HOMO level of styrene (–0.22588 au) and the LUMO level of the active species should refelect the catalytic activity on the basis of the frontier molecular orbital theory. It is generally accepted that the cationic active species of styrene polymerization is the metal center coordinated by the last inserted styrene in η^3-allyl mode and the phenyl ring of penultimate inserted styrene.[26] This allowed us to establish the mode of the active species $[(\text{Flu}-\text{CH}_2-\text{Py})\text{Ln}-(\text{C}_{17}\text{H}_{19})]^+$ where the growing polystyrene chain is simplified as a methyl group and two phenyls of styrene are distributed on both sides of the metal center (Figure 4).

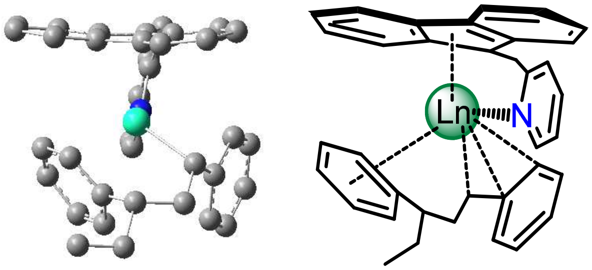

Figure 4. The simulation structure of the active species $[(\text{Flu}-\text{CH}_2-\text{Py})\text{Ln}-(\text{C}_{17}\text{H}_{19})]^+$.

Table 4. Energies of the LUMO of $[(\text{Flu}-\text{CH}_2-\text{Py})\text{Ln}-(\text{C}_{17}\text{H}_{19})]^+$ and energy gaps (ΔE) of HOMO of styrene and LUMO of $[(\text{Flu}-\text{CH}_2-\text{Py})\text{Ln}-(\text{C}_{17}\text{H}_{19})]^+$.[a]

Metal	Sc	Lu	Tm	Er	Ho	Y	Dy	Tb	Gd	Nd	Pr	La
E_{LUMO} (au)	-0.17312	-0.16752	-0.16703	-0.16670	-0.16645	-0.16607	-0.16607	-0.16584	-0.16561	-0.16445	-0.16403	-0.16328
ΔE^{b} (au)	0.05276	0.05885	0.05918	0.05943	0.05962	0.05836	0.05981	0.06004	0.06027	0.06143	0.06185	0.06260
$k_{\text{obs}}\times10^2$ (min^{-1})	12.7	6.0	5.4	5.2	3.6	3.3	2.1	2.1	1.7	0.2	0.1	-

[a] The LUMO energy of $[(\text{Flu}-\text{CH}_2-\text{Py})\text{Ln}-(\text{C}_{17}\text{H}_{19})]^+$ was analyzed on the basis of its optimized geometry afforded via using small core RECPs basic sets; [b] $\Delta E = E_{\text{LUMO(active species)}} - E_{\text{HOMO(Styrene)}}$ ($E_{\text{HOMO(Styrene)}} = –0.22588$ au).

The LUMO energies of $[(\text{Flu}-\text{CH}_2-\text{Py})\text{Ln}-(\text{C}_{17}\text{H}_{19})]^+$ (Ln = Sc, Lu, Tm, Er, Ho, Y, Dy, Tb, Gd, Nd, Pr, La) were analyzed on the basis of its optimized geometry afforded via using small core RECPs basic sets. The results were summarized in

Table 4. The cationic scandium species $[(Flu{-}CH_2{-}Py)Sc{-}(C_{17}H_{19})]^+$ possesses the lowest LUMO energy, leading to the smallest energy gap (ΔE) (0.05276 au) between it and the HOMO energy of styrene. While the LUMO energy of the other cationic rare-earth metal species $[(Flu{-}CH_2{-}Py)Ln{-}(C_{17}H_{19})]^+$ increased from –0.16752 to –0.16328 corresponding to Ln = Lu, Tm, Er, Ho, Y, Dy, Tb, Gd, Nd, Pr and La, respectively, in well consistence with the kinetics behavior of the precursors **1**–**11** (*vide supra*): the lower the LUMO energy is, the higher the activity is. As shown in Figure 5, the LUMOs of the highly active species ($[(Flu{-}CH_2{-}Py)Ln{-}(C_{17}H_{19})]^+$) based on the rare-earth metals varying from Lu to Gd are formed by atomic orbitals (AOs) from the metal, the ligand and the growing polystyrene chain, while those of the low active La, Pr and Nd species have no contribution from the ligand, suggesting that the participation of ligand orbital could reduce the energy of LUMO and therefore make the LUMO energy closer to the HOMO of styrene.

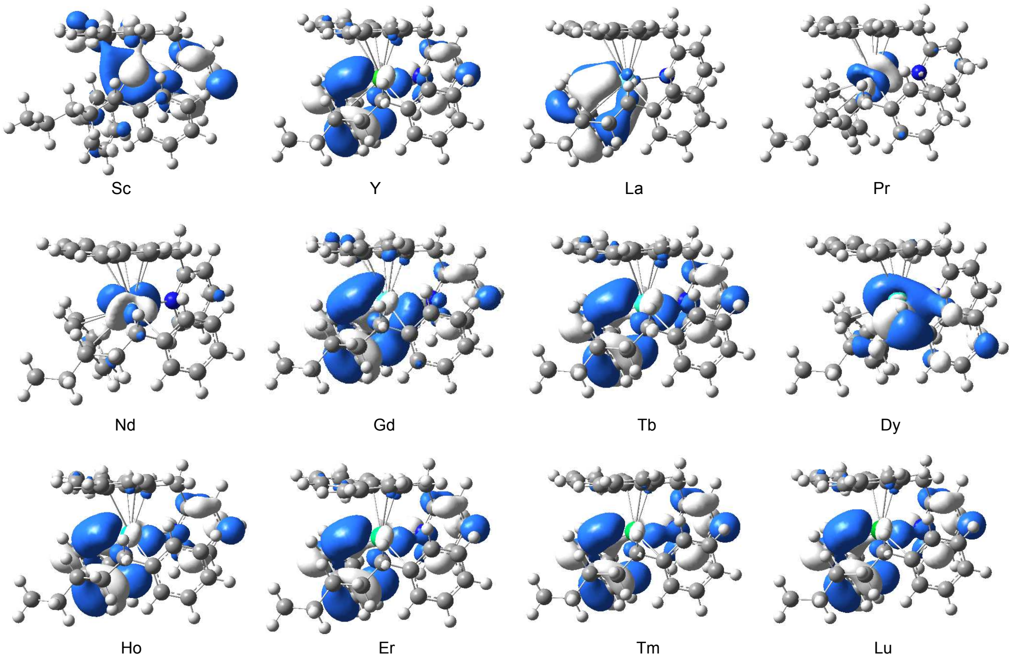

Figure 5. LUMOs of $[(Flu\text{-}CH_2\text{-}Py)Ln{-}(C_{17}H_{19})]^+$ complexes. The isosurface value of the MOs is set to be 0.03 au.

The LUMO energy of the active species could also be used to explain the activity of other catalyst systems for the styrene polymerization. For instance, the LUMO energy of the cationic half-Sandwich rare-earth metal systems

$[(C_5Me_4SiMe_3)Ln{-}(C_{17}H_{19})]^+$ followed the order of Sc < Gd < Y < Lu, in well agreement with the trend of the catalytic activity Sc > Gd > Y > Lu of the experimental results[9] (Figure S10). We synthesized the scandium and yttrium precursors **13** and **14** (Chart 1) bearing the pyridyl-methylene dibenzo[a,i]fluorene ligand, $(Flu^{dibenzo}\text{-}CH_2\text{-}Py)Ln(CH_2SiMe_3)_2(THF)_n$ (Ln = Sc (**13**), n =0; Y (**14**), n = 1), the structurally analogues of **1** and **6**. **13** showed an even higher activity (18 700 kg/(mol(Ln)•h) than **1** because of its low LUMO energy (E_{LUMO}: –0.17425 au), whilst its analogue **14** could only initiate the sluggish polymerization of styrene similar to the Nd active species **10** but much lower than **6** (k_{obs}: 0.4×10^{-2} min^{-1} (**14**) *vs* 0.2×10^{-2} min^{-1} (**10**) *vs* 3.3×10^{-2} min^{-1} (**6**)), in consistence with their LUMO energies (E_{LUMO}: –0.16477(**14**) *vs* –0.16445(**10**) *vs* –0.16607(**6**)).

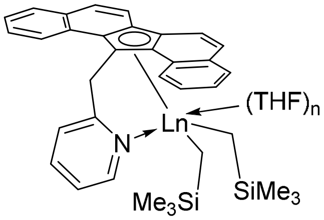

Ln = Sc (**13**), n = 0;
Y (**14**), n = 1

Chart 1. The structures of $(Flu^{dibenzo}\text{-}CH_2\text{-}Py)Sc(CH_2SiMe_3)_2$ (**13**) and $(Flu^{dibenzo}\text{-}CH_2\text{-}Py)Y(CH_2SiMe_3)_2(THF)$ (**14**).

CONCLUSION

Highly active and syndiotactic styrene polymerization catalyzed by the almost entire period of rare earth metals based dialkyl complexes bearing the pyridyl-methylene fluorene ligand except those attached to Nd and Pr elements, has been realized for the first time, which is contributed mainly to the powerful ligand of steric bulkiness and its CGC structure, which provides an opening coordination sphere for styrene monomer. Apparently, the higher the catalytic activity is the smaller the metal size is, in fact, the origin of which is that the orbitals of the ligand participates to form and reduce the LUMO of the active species to facile the coordination of styrene to the active metal species in the cases of small rare-earth metal center proved by the LUMO energy of the active species according to DFT simulation. Hence, the LUMO energy of the active species could be considered as a potential criterion to estimate the catalytic activity of rare-earth metal complexes toward styrene polymerization whenever the styrene coordination being the key step in the polymerization process.

EXPERIMENTAL SECTION

General Methods and Materials. All reactions were carried out under a dry and oxygen-free argon atmosphere by using Schlenk techniques or under a nitrogen atmosphere in an MBraun glovebox. All solvents were purified from an MBraun SPS system. Samples of organo rare-earth metal complexes for NMR spectroscopic measurements were prepared in the glovebox by use of NMR tubes sealed by paraffin film.^{1}H and^{13}C NMR spectra were recorded on a Bruker AV400 or 600 (FT, 400 or 600 MHz for ^{1}H; 100 or 150 MHz for ^{13}C) spectrometer. ^{1}H, ^{13}C NMR spectra of polymer samples were recorded on a Bruker AV400 (FT, 400 MHz for ^{1}H; 100MHz for ^{13}C) spectrometer in tetrachloroethane-d$_2$. The molecular weight and molecular weight distribution of the polymers were measured by means of gel permeation chromatography (GPC) on a PL-GPC 220 type high-temperature chromatography equipped with three PL-gel 10 μm Mixed-B LS type columns at 150 ° C. T_m of polystyrene samples was measured through differential scanning calorimetry (DSC) analyses, which were carried out on a Q 100 DSC from TA Instruments under nitrogen atmosphere. Elemental analyses were performed at National Analytical Research Centre of Changchun Institute of Applied Chemistry (CIAC). Styrene was dried over CaH2 under stirring for 48 h and distilled under reduced pressure before use. ^{n}BuLi (2.5 M in hexane) was purchased from Aldrich. $[Ph_3C][B(C_6F_5)_4]$ was prepared following the literature procedures.[27]

DFT calculations. All the DFT calculations were performed with the Gaussian 09 program.[28] The B3PW91 hybrid exchange-correlation functional was utilized. In the geometry optimizations and subsequent analytical frequency calculations, the 6-31G* basis set was used for H, C, O, and N atoms, and the relativistic effective core potentials (RECPs) developed by the Stuttgart/Dresden group for Si and rare-earth metal atoms were used. Geometries of all the species were fully optimized without symmetry constrains. Population analyses were carried out to the natural bond orbital (NBO) formalism. The TSs were characterized by a single imaginary frequency for the correct mode. The stable species (minima) were verified to have all real frequencies only.

X-ray Crystallographic Studies. Crystals for X-ray analysis were obtained as described in the preparations. The crystals were manipulated in a glovebox. Data collections were performed at –88.5 ^{o}C on a Bruker SMART APEX diffractometer with a CCD area detector, using graphite-monochromated Mo Kα radiation (λ = 0.71073 Å). The determination of crystal class and unit cell parameters was carried out by the SMART program package. The raw frame data were processed using SAINT and SADABS to yield the reflection data file. The structures were solved by using the SHELXTL program. Refinement was performed on F^2 anisotropically for all non-hydrogen atoms by the full-matrix least-squares method. The hydrogen atoms were placed at the calculated positions and were included in the structure calculation without further refinement of the parameters.

Synthesis of dibenzo[*a*,*i*]FluCH$_2$-Py.

For the preparation of di(naphthalen-1-yl)methanol, a modification of the procedure reported by Koskinen[29] was used. A solution of 41.4 g (200 mmol) of 1-bromonaphthalene in 100 mL of THF was dropped within 20 min into a 5.1 g (210 mmol) of magnesium turnings in 100mL THF under vigorous stirring. The reaction was stirred for 4h at 70 °C. Subsequently, a solution of 6.1 mL (100 mmol) of methyl formate in 25 mL of THF was added to the reaction mixture within 20 min. After the reaction mixture was stirred for 2h under 70 °C, volatile compounds were removed under reduced pressure. The residue was dissolved in Et$_2$O (500 mL) and the organic layer was washed with 1 M HCl (500 mL), H$_2$O (500 ml) and saturated NaCl (500 mL). After the Et_2O layer was dried over $MgSO_4$, the volatile compounds were removed under reduced pressure, then the residue was scattered by hexane (500 mL) and stirred overnight, filtered and washed with cold hexane, then the filter cake was dried under vacuum to give di(naphthalen-1-yl)methanol as a white powder with satisfactory purity (27.0 g, 95%).

Colorless suspension of di(naphthalen-1-yl)methanol (27.0 g, 95 mmol) in 150 ml of PPA(polyphosphoric acid) was heated at 180 °C for 6 h. Subsequently, $CHCl_3$ (1000 mL) and water (1000 mL) was added to the dark green reaction mixture, and organic layer was separated, washed with a saturated Na_2CO_3 aqueous solution followed by a saturated NaCl aqueous solution. The organic layer dried over $MgSO_4$ and the volatile compounds were removed under reduced pressure. Sublimation of the resultant solid reside at 180 °C gave dibenzo[*a*,*i*]fluorene as a white or pale yellow solid(10.6 g, 42%).^{1}H NMR (400 MHz, $CDCl_3$, 25℃) δ 8.13 (d, *J* = 8.3 Hz, 2H, Ar-H), 7.99 (d, *J* = 8.4 Hz, 2H, Ar-H), 7.92 (t, *J* = 8.0 Hz, 4H, Ar-H), 7.55-7.59 (m, 2H, Ar-H), 7.44-7.49 (m, 2H, Ar-H), 4.49 (s, 2H, CH_2).

Under a nitrogen atmosphere, dibenzo[*a*,*i*]fluorene (40 mmol, 10.6 g) dissolve in dry Et_2O (100 mL), ^{n}BuLi (2.5 M in hexane) (42 mmol, 17 mL)was add dropwise to the Et_2O solution under -78 °C and stirred for 2 h under this temperature. The reaction system was slowly heated to room temperature and stirred for another 2 h. At the same time Py-CH_2Cl was dissolved in dry Et_2O (50 mL), and the Et_2O solution of dibenzo[*a*,*i*]Flu-Li was added dropwise to Py-CH_2Cl slowly under -30 °C. After the reaction mixture was stirred for 12 h under -30 °C, the reaction mixture is poured into 200 mL of saturated NH_4Cl, and the Et_2O layer was washed with 200 ml water for three times. After the organic layer was dried over $MgSO_4$ overnight, volatile compounds were removed under reduced pressure. After the residue was purified with column chromatography (silica gel, Petroleum ether/ Ethyl acetate, 10:1, v/v), dibenzo[*a*,*i*]FluCH_2-Py was gave as white or pale green powders.

^{1}H NMR (400 MHz, $CDCl_3$) δ 8.55 (d, *J* = 12.8 Hz, 1H, Py-H), 7.78-7.93 (m, 8H, Ar-H), 7.35-7.42 (m, 4H, Ar-H), 7.22 (dt, *J* = 7.6, 1.8 Hz, 1H, Py-H), 7.02-7.11 (m, 1H, Py-H), 6.42 (d, *J* = 7.7 Hz, 1H, Py-H), 5.43 (t, *J* = 5.9 Hz, 1H, CH), 3.52 (d, *J* = 5.9 Hz, 2H, CH_2). ^{13}C NMR (101 MHz, $CDCl_3$) δ 159.30, 149.32, 144.69, 138.71, 135.76, 133.06, 130.13, 129.08, 128.28, 126.14, 124.91, 124.67, 124.25, 121.36, 118.56, 46.69, 43.72.

General Procedure for the Preparation of Complexes (Flu-CH_2-Py)Ln(CH_2SiMe_3)$_2$(THF)$_n$. Under a nitrogen atmosphere, Flu-CH_2-Py(1.0 equiv) reacted with 1.0 equiv of ^{n}BuLi in the mixture solvent of toluene and THF (Tol/THF = 10/1) to give a red [Py-CH_2-Flu]Li solution. And, to a suspension of $LnCl_3$ (1.0 equiv) in mixed solvents of toluene and THF (Tol/THF = 10/1), 1 equiv of [Py-CH_2-Flu]Li solution was slowly added at room temperature. The mixture was stirred for 8 h to afford a yellow suspension, to which $LiCH_2SiMe_3$ (2.0 equiv) was added and the resulting suspension was stirring overnight to afford a yellowish-brown solution (-30 °C). Removal of volatile compounds, extraction with toluene, and recrystallization under -30 °C gave complex as crystalline solid and the crystal was suitable for X-ray analysis.

Synthesis of Complex (FluCH$_2$-Py)Tm(CH$_2$SiMe$_3$)$_2$(THF)(3). According to the general procedure mentioned above, $TmCl_3$ (1 mmol, 0.28 g) was reacted with [Py-CH_2-Flu]Li for 8h and then added $LiCH_2SiMe_3$(2 mmol, 0.19 g) to react over night at room temperature to afford **4** as yellow powders(0.56 g, 83.1%). Anal. calcd for $C_{31}H_{44}NTmSi_2O$ (%): C, 55.42; H, 6.60; N, 2.08. Found: C, 55.22; H, 6.51; N, 2.02.

Synthesis of Complex (FluCH$_2$-Py)Er(CH$_2$SiMe$_3$)$_2$(THF)(4). According to the general procedure, $ErCl_3$ (1 mmol, 0.27 g) was reacted with [Py-CH_2-Flu]Li for 8h and then added $LiCH_2SiMe_3$(2 mmol, 0.19 g) to react over night at room temperature to afford **5** as yellow powders (0.54 g, 80.2%). The identity of the product was corroborated by single crystal X-ray diffraction. Anal. calcd for $C_{31}H_{44}NErSi_2O$ (%): C, 55.56; H, 6.62; N, 2.09. Found: C, 55.12; H, 6.21; N, 2.01.

Synthesis of Complex (FluCH$_2$-Py)Ho(CH$_2$SiMe$_3$)$_2$(THF)(5). According to the general procedure, $HoCl_3$ (1 mmol, 0.27 g) was reacted with [Py-CH_2-Flu]Li for 8h and then added $LiCH_2SiMe_3$(2 mmol, 0.19 g) to react over night at room temperature to afford **6** as yellow powders (0.54 g, 80.6%). Anal. calcd for $C_{31}H_{44}NHoSi_2O$ (%): C, 55.76; H, 6.64; N, 2.10. Found: C, 55.12; H, 6.41; N, 2.07.

Synthesis of Complex (FluCH$_2$-Py)Dy(CH$_2$SiMe$_3$)$_2$(THF)(7). Following the above procedure, $DyCl_3$ (1 mmol, 0.27 g) was reacted with [Py-CH$_2$-Flu]Li for 8h and then added $LiCH_2SiMe_3$(2 mmol, 0.19 g) to react over night at -30 °C to afford **7** as yellow powders (0.52 g, 78.6%). Anal. calcd for $C_{31}H_{44}NDySi_2O$ (%): C, 55.96; H, 6.67; N, 2.11. Found: C, 55.27; H, 6.41; N, 2.09.

Synthesis of Complex (FluCH$_2$-Py)Tb(CH$_2$SiMe$_3$)$_2$(THF)(8). Following the above procedure, $TbCl_3$ (1 mmol, 0.26 g) was reacted with [Py-CH$_2$-Flu]Li for 8h and then added $LiCH_2SiMe_3$(2 mmol, 0.19 g) to react over night at -30 °C to afford **8** as yellow powders (0.51 g, 76.4%). Anal. calcd for $C_{31}H_{44}NTbSi_2O$ (%): C, 56.26; H, 6.70; N, 2.12. Found: C, 55.87; H, 6.53; N, 2.09.

Synthesis of Complex (FluCH$_2$-Py)Gd(CH$_2$SiMe$_3$)$_2$(THF)(9). Following the above procedure, $GdCl_3$ (1 mmol, 0.26 g) was reacted with [Py-CH$_2$-Flu]Li for 8h and then added $LiCH_2SiMe_3$ (2 mmol, 0.19 g) to react over night at -30 °C to afford **9** as yellow powders (0.47 g, 72.1%).The identity of the product was corroborated by single crystal X-ray diffraction. Anal. calcd for $C_{31}H_{44}NGdSi_2O$ (%): C, 55.56; H, 6.62; N, 2.09. Found: C, 55.12; H, 6.21; N, 2.01.

Synthesis of Complex (FluCH$_2$-Py)Nd(CH$_2$SiMe$_3$)$_2$(THF)(10). Following the above procedure, $NdCl_3$ (1 mmol, 0.25 g) was reacted with [Py-CH$_2$-Flu]Li for 8h and then added $LiCH_2SiMe_3$ (2 mmol, 0.19 g) to react over night at -30 °C to afford **10** as yellow powders (0.19 g, 30%).The identity of the product was corroborated by single crystal X-ray diffraction. Anal. calcd for $C_{31}H_{44}NNdSi_2O$ (%): C, 57.54; H, 6.85; N, 2.16. Found: C, 57.04; H, 6.51; N, 2.11.

Synthesis of Complex (FluCH$_2$-Py)Pr(CH$_2$SiMe$_3$)$_2$(THF)(11). Following the above procedure, $PrCl_3$ (1 mmol, 0.25 g) was reacted with [Py-CH$_2$-Flu]Li for 8h and then added $LiCH_2SiMe_3$ (2 mmol, 0.19 g) to react over night at -30 °C to afford **11** as yellow powders (0.16 g, 50.2%). The identity of the product was corroborated by single crystal X-ray diffraction. Anal. calcd for $C_{31}H_{44}NPrSi_2O$ (%): C, 57.84; H, 6.89; N, 2.18. Found: C, 56.63; H, 6.43; N, 2.16.

Synthesis of Complex (FluCH$_2$-Py)$_2$La(CH$_2$SiMe$_3$) (12). Following the above procedure, LaCl$_3$ (1 mmol, 0.24 g) was reacted with [Py-CH$_2$-Flu]Li for 8h and then added LiCH$_2$SiMe$_3$ (2 mmol, 0.19 g) to react over night at -30 °C to afford **12** as yellow powders (0.08 g, 10%). ^{1}H NMR (400 MHz, C_6D_6, 25 °C): δ –2.82 (d, $^2J_{H,H}$ = 9.3 Hz, 1 H, La-CH_2SiMe$_3$), –1.70 (d, $^2J_{H,H}$ = 9.3 Hz, 1 H, La-CH_2SiMe$_3$), –0.05 (s, 9 H, La-CH$_2$SiMe_3), 1.38 (br s, 4H, THF), 3.58 (br s, 4H, THF), 3.76 (d, $^2J_{H,H}$ = 18.0 Hz, 2 H, PyCH_2), 3.76 (d, $^2J_{H,H}$ = 18.0 Hz, 2 H, PyCH_2), 6.47 (t, $^3J_{H,H}$ = 7.5 Hz, 1H, C$_5H_4$N), 6.53 (d, $^3J_{H,H}$ = 8.3 Hz, 1H, C$_5H_4$N), 6.59 (t, $^3J_{H,H}$ = 6.6 Hz, 1H, C$_5H_4$N), 6.73 (d, $^3J_{H,H}$ = 7.9 Hz, 1H, C$_5H_4$N), 6.94-7.15 (m, 2H, C$_5H_4$N 14H, C$_{13}H_8$), 7.23 (t, $^3J_{H,H}$ = 7.2 Hz, 1H, C$_{13}H_8$),7.40 (d, $^3J_{H,H}$ = 7.1 Hz, 1H, C$_{13}H_8$), 7.96 (d, $^3J_{H,H}$ = 8.0 Hz, 1H, C$_5H_4$N), 8.33 (d, $^3J_{H,H}$ = 5.0 Hz, 1H, C$_5H_4$N). Anal. calcd for $C_{46}H_{47}N_2LaSiO$ (%): C, 68.14; H, 5.84; N, 3.45. Found: C, 68.12; H, 5.86; N, 3.44.

Synthesis of Complex (dibenzo[*a*,*i*]FluCH$_2$-Py)Sc(CH$_2$SiMe$_3$)$_2$ (13). Following the above procedure, ScCl$_3$(THF)$_3$ (1 mmol, 0.37 g) was reacted with [dibenzo[*a*,*i*]Flu]Li for 8h and then LiCH$_2$SiMe$_3$(2 mmol, 0.19 g) was added to react over night at -30 °C to afford the product as yellow powders of **13** (0.49 g, 85%). ^{1}H NMR (400 MHz, C_6D_6) δ 8.28 (d, J = 5.2 Hz, 1H, Py-H), 8.20 (d, J = 8.99 Hz, 2H, Ar-H), 8.10-8.15 (m, 2H, Ar-H), 7.80-7.82 (m, 2H, Ar-H), 7.55 (d, J = 8.9 Hz, 2H, Ar-H), 7.32-7.21 (m, 4H, Ar-H), 6.84 (td, J = 7.8, 1.6 Hz, 1H), 6.74 (d, J = 8.0 Hz, 1H), 6.27-6.20 (m, 1H), 5.18 (s, 2H), 2.11 (s, 1H), -0.13 (s, 18H), -0.96 (d, J = 3.1 Hz, 4H). ^{13}C NMR (100 MHz, C_6D_6) δ 169.16, 155.55, 138.13, 132.41, 135.68, 131.91, 126.06, 123.22, 122.90, 122.47, 122.02, 123.67, 121.69, 121.48, 120.31, 116.39, 100.07, 34.65, 25.96. Anal. calcd for $C_{39}H_{48}NYSi_2O$ (%): C, 73.00; H, 7.00; N, 2.43. Found: C, 73.12; H, 7.03; N, 2.36.

Synthesis of Complex (dibenzo[*a*,*i*]FluCH$_2$-Py)Y(CH$_2$SiMe$_3$)$_2$(THF) (14). Following the above procedure, YCl$_3$ (1 mmol, 0.20 g) was reacted with [dibenzo[*a*,*i*]Flu]Li for 8h and then added LiCH$_2$SiMe$_3$ (2 mmol, 0.19 g) to react over night at -30 °C to afford the product **14** (0.47 g, 68%). Recrystallization from hexane and toluene gave single crystals suitable for X-ray analysis. ^{1}H NMR (400 MHz, C_6D_6) δ 8.82 (d, J = 5.2 Hz, 1H, Py-H), 8.23 (dd, J = 8.6, 4.2 Hz, 2H, Ar-H), 7.85-7.91 (m, 4H, Ar-H), 7.44 (d, $J = 8.8$ Hz, 2H, Ar-H), 7.29-7.33(m, 4H, Ar-H), 7.02 (dd, $J = 7.3$, 5.7 Hz, 1H, Py-H), 6.89-6.96 (m, 1H, Py-H), 6.64 (dd, $J = 14.0$, 7.1 Hz, 1H, Py-H), 5.36 (S, 2H, CH_2), 3.50 (s, 4H, THF), 1.37 (s, 4H, THF), -0.18 (s, 18H, $CH_2Si\mathit{Me_3}$), -1.74 (d, $J = 2.6$ Hz, 4H, $\mathit{CH_2}SiMe_3$). ^{13}C NMR (100 MHz, C_6D_6) δ 167.06, 150.55, 138.73, 133.41, 130.68, 129.71, 128.06, 126.02, 124.90, 124.47, 124.02, 123.87, 121.89, 121.68, 120.35, 116.99, 103.07, 71.15, 39.49, 37.65, 25.16. Anal. calcd for $C_{39}H_{48}NYSi_2O$ (%): C, 67.70; H, 7.99; N, 2.02. Found: C, 68.65; H, 7.63; N, 2.26.

Typical Procedure for Styrene Polymerization. A typical polymerization procedure is as follow (Table 2, entry 1): In a glove box, 10.4 g (100 mmol) of styrene was added into a toluene solution (50 ml) of Al^iBu_3(50 μmol) in 100 mL flask. Then, a toluene solution (7 mL) of **1** (5.4 mg, 10 μmol), 1 equiv $[Ph_3C][B(C_6F_5)_4]$ (9.2 mg, 10 μmol) and Al^iBu_3 (50 μmol) was added to the flask. After stirring for 60 min (the magnetic stirring was ceased within a few minutes), methanol was injected to terminate the polymerization. The viscous mixture was poured into a large quantity of methanol to precipitate the polymer product. The obtained white polymer was filtered and then dried under vacuum at 40 °C to a constant weight.

Typical Procedure for Kinetic Experiment of Styrene Polymerization. A typical kinetic experiment procedure is as follow: In a glove box, 2.08 g (20 mmol) of styrene was added into a toluene solution (50 ml) of Al^iBu_3 (25 μmol) in 100 mL flask. Then, a toluene solution (5 mL) of rare-earth metal complex (10 μmol), 1 equiv $[Ph_3C][B(C_6F_5)_4]$ (9.2 mg, 10 μmol) and Al^iBu_3 (25 μmol) was added to the flask. The polymerization mixture was divided into six portions to six bottles, respectively. After stirring for different times, methanol was injected to terminate the polymerization systems. The viscous mixtures were poured into a large quantity of methanol to precipitate the polymer products. The obtained white polymers were filtered and then dried under vacuum at 40 °C to constant weights, The conversion was calculated by weight.

ASSOCIATED CONTENT

Supporting Information

X-ray structures of complexes **4**, **9** and **10**; Plot of $\ln([St]_0/[St]_t)$ vs. time catalyzed by complexes **1-11** under activation of $[Ph_3C][B(C_6F_5)_4]$ and Al^iBu_3; The molecular structure of the ion pair of (Flu−CH_2−Py)Sc(CH_2SiMe_3)$^+$[B(C_6H_6)$_4$]$^-$ simulated by DFT calculation; LUMOs of [($C_5Me_4SiMe_3$)Ln($C_{17}H_{19}$)(THF)]$^+$ complexes; Selected bond distances (Å) and angles (deg) of complexes **2**, **4**, **9**, **10** and **11**; Representative GPC-traces, DSC-traces, and NMR spectra of the polymers. These information are available free of charge via the Internet at http://pubs.acs.org.

AUTHOR INFOEMATION

Corresponding Authors

* (D.C.) E-mail: dmcui@ciac.ac.cn. Fax: (+86) 431 85262774. Telephone: +86 431 85262773.

* (B.L.) E-mail: liubo@ciac.ac.cn.

* (Y.L.) E-mail: luoyi@dlut.edu.cn.

Notes

The authors declare no competing financial interest.

ACHNOWLEDGMENTS

This work was supported by the NSF China for Projects Nos. 21374112 and 21174023, and MST for “973” project No. 2015CB654700. The authors are grateful to Computing Center of Jilin Province for essential support.

REFERENCES

(1) (a) Cotton, S. A. *Scandium, Yttrium & the Lanthanides: Inorganic & Coordination Chemistry*. In *Encyclopedia of Inorganic Chemistry*; John Wiley & Sons, Ltd: Chichester, UK. 2006; p 2. (b) Shannon, R. *Acta Crystallogr., Sect. A: Found.* **1976**, *32*, 751-767.

(2) Arndt, S.; Spaniol, T. P.; Okuda, J. *Angew. Chem., Int. Ed.* **2003**, *42*, 5075-5079.

(3) Bambirra, S.; Bouwkamp, M. W.; Meetsma, A.; Hessen, B. *J. Am. Chem. Soc.* **2004**, *126*, 9182-9183.

(4) Yasuda, H.; Yamamoto, H.; Yamashita, M.; Yokota, K.; Nakamura, A.; Miyake, S.; Kai, Y.; Kanehisa, N. *Macromolecules* **1993**, *26*, 7134-7143.

(5) Salzinger, S.; Soller, B. S.; Plikhta, A.; Seemann, U. B.; Herdtweck, E.; Rieger, B. *J. Am. Chem. Soc.* **2013**, *135*, 13030-13040.

(6) (a) Ishihara, N.; Kuramoto, M.; Uoi, M. *Macromolecules* **1988**, *21*, 3356-3360. (b) Ishihara, N.; Seimiya, T.; Kuramoto, M.; Uoi, M. *Macromolecules* **1986**, *19*, 2464-2465.

(7) (a) Hafner, A.; Okuda, J. *Organometallics* **1993**, *12*, 949-950. (b) Ready, T. E.; Day, R. O.; Chien, J. C. W.; Rausch, M. D. *Macromolecules* **1993**, *26*, 5822-5823. (c) Schroder, K.; Haase, D.; Saak, W.; Lutzen, A.; Beckhaus, R. *Organometallics* **2006**, *25*, 3824-3836. (d) Xu, G. X.; Cheng, D. L. *Macromolecules* **2000**, *33*, 2825-2831.

(8) Kirillov, E.; Lehmann, C. W.; Razavi, A.; Carpentier, J. F. *J. Am. Chem. Soc.* **2004**, *126*, 12240-12241.

(9) Luo, Y. J.; Baldamus, J.; Hou, Z. M. *J. Am. Chem. Soc.* **2004**, *126*, 13910-13911.

(10) (a) Bonnet, F.; Violante, C. D.; Roussel, P.; Mortreux, A.; Visseaux, M. *Chem. Commun.* **2009**, 3380-3382. (b) Luo, Y. J; Feng, X.; Wang, Y.; Fan, S.; Chen, J.; Lei, Y.; Liang, H. *Organometallics* **2011**, *30*, 3270-3274.

(11) (a) Hitzbleck, J.; Beckerle, K.; Okuda, J. *J. Organomet. Chem.* **2007**, *692*, 4702-4707. (b) Hitzbleck, J.; Okuda, J. *Z. Anorg. Allg. Chem* **2006**, *632*, 1947-1949. (c) Luo, Y. J.; Chi, S. H.; Chen, J. *New J Chem* **2013**, *37*, 2675-2682.

(12) (a) Fang, X. D.; Li, X. F.; Hou, Z. M.; Assoud, J. L.; Zhao, R. *Organometallics* **2009**, *28*, 517-522. (b) Jaroschik, F.; Shima, T.; Li, X. F.; Mori, K.; Ricard, L.; Le Goff, X. F.; Nief, F.; Hou, Z. M. *Organometallics* **2007**, *26*, 5654-5660. (c) Nishiura, M.; Mashiko, T.; Hou, Z. M. *Chem. Commun.* **2008**, 2019-2021.

(13) (a) Xu, X.; Chen, Y. F.; Sun, J. *Chem. Eur. J.* **2009**, *15*, 846-850. (b) Lei, Y. L.; Wang, Y. B.; Luo, Y. J. *J Organomet Chem* **2013**, *738*, 24-28.

(14) Li, X. F.; Wang, X. Y.; Tong, X.; Zhang, H. X.; Chen, Y. Y.; Liu, Y.; Liu, H.; Wang, X. J.; Nishiura, M.; He, H.; Lin, Z. G.; Zhang, S. W.; Hou, Z. M. *Organometallics* **2013**, *32*, 1445-1458.

(15) (a)Jian, Z. B.; Tang, S. J.; Cui, D. M. *Chem. Eur. J.* **2010**, *16*, 14007-14015. (b) Jian, Z. B.; Tang, S. J.; Cui, D. M. *Macromolecules* **2011**, *44*, 7675-7681.

(16) Pan, Y. P.; Rong, W. F.; Jian, Z. B.; Cui, D. M. *Macromolecules* **2012**, *45*, 1248-1253.

(17) Jian, Z. B.; Cui, D. M.; Hou, Z. M. *Chem. Eur. J.* **2012**, *18*, 2674-2684.

(18) Altenbuchner, P. T.; Soller, B. S.; Kissling, S.; Bachmann, T.; Kronast, A.; Vagin, S. I.; Rieger, B. *Macromolecules* **2014**, *47*, 7742-7749.

(19) (a) Chen, E. Y. X.; Marks, T. J. *Chem. Rev.* **2000**, *100*, 1391-1434. (b) Jordan, R. F.; Lapointe, R. E.; Bajgur, C. S.; Echols, S. F.; Willett, R. *J. Am. Chem. Soc.* **1987**, *109*, 4111-4113. (c) Lin, Z. R.; Lemarechal, J. F.; Sabat, M.; Marks, T. J. *J. Am. Chem. Soc.* **1987**, *109*, 4127-4129. (d) Stapleton, R. A.; Galan, B. R.; Collins, S.; Simons, R. S.; Garrison, J. C.; Youngs, W. J. *J. Am. Chem. Soc.* **2003**, *125*, 9246-9247.

(20) The signal of methene within $Ph_3CCH_2SiMe_3$ was found at 2.27 ppm, which is comparable to the literature: Luo, Y. J.; Baldamus, J.; Hou, Z. M. *J. Am. Chem. Soc.* **2004**, *126*, 13910-13911. indicating that the formation of the ion pairs.

(21) (a) Baumann, R.; Davis, W. M.; Schrock, R. R. *J. Am. Chem. Soc.* **1997**, *119*, 3830-3831. (b) Yu, N.; Nishiura, M.; Li, X. F.; Xi, Z. F.; Hou, Z. M. *Chem. Asian. J.* **2008**, *3*, 1406-1414.

(22) Voth, P.; Arndt, S.; Spaniol, T. P.; Okuda, J.; Ackerman, L. J.; Green, M. L. H. *Organometallics* **2003**, *22*, 65-76.

(23) (a) Horton, A. D.; Frijns, J. H. G. *Angew. Chem. Int. Ed.* **1991**, *30*, 1152-1154. (b) Pasquali, M.; Floriani, C.; Gaetanimanfredotti, A. *Inorg. Chem.* **1980**, *19*, 1191-1197.

(24) The integral intensity ratio of the resonance at 8.02, 7.90, 7.09, 7.01, 6.75 is 1:1:1:1:1, while the integral intensity ratio of the resonance at 7.55, 6.90, 6.78 is 6:6:3.

(25) Matsui, S.; Mitani, M.; Saito, J.; Tohi, Y.; Makio, H.; Matsukawa, N.; Takagi, Y.; Tsuru, K.; Nitabaru, M.; Nakano, T.; Tanaka, H.; Kashiwa, N.; Fujita, T. *J. Am. Chem. Soc.* **2001**, *123*, 6847-6856.

(26) (a) Perrin, L.; Sarazin, Y.; Kirillov, E.; Carpentier, J. F.; Maron, L. *Chem. Eur. J.* **2009**, *15*, 3773-3783. (b) Minieri, G.; Corradini, P.; Guerra, G.; Zambelli, A.; Cavallo, L. *Macromolecules* **2001**, *34*, 5379-5385. (c) Minieri, G.; Corradini, P.; Zambelli, A.; Guerra, G.;

Cavallo, L. *Macromolecules* **2001**, *34*, 2459-2468. (d) Perrin, L.; Kirillov, E.; Carpentier, J.-F.; Maron, L., *Macromolecules* **2010**, *43*, 6330-6336.

(27) (a) Tjaden, E. B.; Swenson, D. C.; Jordan, R. F.; Petersen, J. L. *Organometallics* **1995**, *14*, 371-386. (b) Chien, J. C. W.; Tsai, W. M.; Rausch, M. D. *J. Am. Chem. Soc.* **1991**, *113*, 8570-8571.

(28) Frisch, M. J., Trucks, G. W., Schlegel, H. B., Scuseria, G. E., Robb, M. A., Cheeseman, J. R., Scalmani, G., Barone, V., Mennucci, B., Petersson, G. A., Nakatsuji, H., Caricato, M., Li, X., Hratchian, H. P., Izmaylov, A. F., Bloino, J., Zheng, G., Sonnenberg, J. L., Hada, M., Ehara, M., Toyota, K., Fukuda, R., Hasegawa, J., Ishida, M., Nakajima, T., Honda, Y., Kitao, O., Nakai, H., Vreven, T., Montgomery, J. A., Peralta, J. E. Jr., Ogliaro, F., Bearpark, M., Heyd, J. J., Brothers, E., Kudin, K. N., Staroverov, V. N., Kobayashi, R., Normand, J., Raghavachari, K., Rendell, A., Burant, J. C., Iyengar, S. S., Tomasi, J., Cossi, M., Rega, N., Millam, J. M., Klene, M., Knox, J. E., Cross, J. B., Bakken, V., Adamo, C., Jaramillo, J., Gomperts, R., Stratmann, R. E., Yazyev, O., Austin, A. J., Cammi, R., Pomelli, C., Ochterski, J. W., Martin, R. L., Morokuma, K., Zakrzewski, V. G., Voth, G. A., Salvador, P., Dannenberg, J. J., Dapprich, S., Daniels, A. D., Farkas, O., Foresman, J. B., Ortiz, J. V., Cioslowski, J., and Fox, D. J. (2009) *Gaussian 09*, revision A.02; Gaussian, Inc., Wallingford, CT.

(29) Bassas, O.; Huuskonen, J.; Rissanen, K.; Koskinen, A. M. P. *Eur. J. Org. Chem.* **2009**, 1340-1351.

Nature of the Entire Range of Rare-Earth Metal Based Cationic Catalysts for Highly Active and Syndioselective Styrene Polymerization

Fei Lin[1,2], Xingbao Wang[3], Yupeng Pan[1,2], Meiyan Wang[4], Bo Liu,[1]* Yi Luo,[3*] and Dongmei Cui [1]*

[1]State Key Laboratory of Polymer Physics and Chemistry, Changchun Institute of Applied Chemistry, Chinese Academy of Sciences, Changchun 130022, China

[2]University of the Chinese Academy of Sciences, Changchun Branch, Changchun 130022, China

[3]State Key Laboratory of Fine Chemicals, School of Pharmaceutical, Science and Technology, Dalian University of Technology, Dalian 116024, China

[4]Institute of Theoretical Chemistry, State Key Laboratory of Theoretical and Computational Chemistry, Jilin University, Changchun 130022, China

*Corresponding authors: FAX +86 431 85262774; e-mail dmcui@ciac.ac.cn; liubo@ciac.ac.cn; luoyi@dlut.edu.cn